

Split-bolus MR urography: synchronous visualization of obstructing vessels and collecting system in children

Bilal Battal
Murat Kocaoğlu
Veysel Akgün
Selami İnce
Faysal Gök
Mustafa Taşar

ABSTRACT

Several vascular abnormalities related with urinary system such as crossing accessory renal vessels, retroiliac ureters, retrocaval ureters, posterior nutcracker syndrome, and ovarian vein syndrome may be responsible for urinary collecting system obstruction. Split-bolus magnetic resonance urography (MRU) using contrast material as two separate bolus injections provides superior demonstration of the collecting system and obstructing vascular anomalies simultaneously and enables accurate preoperative radiologic diagnosis. In this pictorial review we aimed to outline the split-bolus MRU technique in children, list the coexisting congenital collecting system and vascular abnormalities, and exhibit the split-bolus MRU appearances of concurrent urinary collecting system and vascular abnormalities.

Magnetic resonance urography (MRU) is a noninvasive imaging technique that does not involve ionizing radiation or iodinated contrast medium. Therefore, it has a potential to noninvasively illustrate various urinary tract abnormalities and provides both morphologic and functional information. MRU can be obtained by two different techniques: T2-weighted MRU (also known as static-fluid MRU) and T1-weighted MRU (also known as contrast-enhanced excretory MRU) (1–3). Generally used contrast-enhanced MRU protocol with single-bolus contrast material injection consists of dynamic scanning of urinary system at different phases. However, using the single bolus technique, vessels and collecting systems cannot be demonstrated simultaneously. Although split bolus computed tomography (CT) urography is widely used in adults and described in the literature, the major disadvantage in multiphasic scans and follow-up is the radiation exposure, particularly in pediatric patients who are more susceptible to radiation-related effects including cancer and mutations. Compared with adults, children are considerably more sensitive to radiation and have a longer life expectancy resulting in a larger window for expressing radiation damage (4). Moreover, the administration of potentially nephrotoxic iodinated contrast agents in this group that are prone to renal impairment is an important restriction for CT urography (2).

In this article, we aimed to summarize the MRU technique with the emphasis on split-bolus MRU and its role in demonstrating vascular anomalies related with urinary collecting system.

MRU technique

MRU can provide both morphologic and functional information about the urinary tract using two-dimensional (2D) and three-dimensional (3D) T1- and T2-weighted sequences. The 2D T1- and T2-weighted sequences are suitable for morphologic assessment of the urinary system. MRU technique uses the fast gradient echo 3D T1-weighted magnetic resonance imaging (MRI) sequences to obtain urographic images. With the administration of gadolinium-based contrast agent via intravenous (i.v.) route, i.v. urography-like images can be obtained by employing the maximum intensity projection (MIP) method. When the urinary system is imaged during the arterial, parenchymal, and excretory phases, contrast-enhanced MRI allows evaluation of the kidneys and ureters, as well as renal vasculature (Fig. 1). In this technique, differential renal function can also be calculated by using the time-signal intensity curves (1–3, 5).

On the other hand, T2-weighted 3D MRU simply depicts the static fluid. It uses urine as an intrinsic contrast medium and does not require i.v. contrast medium. Therefore, it is in-

From the Departments of Radiology (B.B., V.A., S.İ. M.T.) and Pediatric Nephrology (F.G.), Gülhane Military Medical School, Ankara, Turkey; the Department of Radiology (M.K. ✉ drmuratkocaoglu@gmail.com), Near East University School of Medicine, Nicosia, Northern Cyprus.

Received 12 February 2015; revision requested 25 March 2015; revision received 31 March 2015; accepted 21 April 2015.

Published online 31 August 2015.
DOI 10.5152/dir.2015.15068

dependent of renal function and can be used to evaluate dilated urinary system in poorly functioning or nonfunctioning kidneys. T2-weighted MRU is an important tool to demonstrate urinary system pathologies in childhood because of high contrast resolution and no radiation. T2-weighted MRU images can be obtained as a single thick slab or MIP views generated from multiple thin slice 3D T2-weighted images (1–3, 5); but, T2-weighted sequences do not provide functional information (Fig. 2).

For MRU studies, patients are hydrated with saline infusion starting 30 minutes prior to examination. The children under the age of seven years may require i.v. sedation or general anesthesia. MRU examinations can be performed with either 1.5 T or 3.0 T MRI scanners using phased-array body coils. MRU protocol begins with localizing sequences and continues with conventional axial and coronal 2D T1 and T2-weighted MRI sequences to assess the renal parenchyma and periurinary area. Then MRU protocol continues with thick-slab single and multislice 3D T2-weighted MRU sequences. Subsequently, 0.3 mg/kg furosemide and 0.1 mmol/kg of gadolinium-based contrast agent are given intravenously at the same time. There have been different timing techniques of gadolinium and furosemide injection. Furosemide has been injected before, after, or at the same time with gadolinium on different studies. We obtained good opacification with the latter technique and avoided patient discomfort due to early bladder filling. Furosemide is admin-

istered to dilate the collecting system by increasing glomerular filtration rate and to reduce the T2* effect of intravenously administered contrast agent. Patients are examined in the coronal plane during the vascular and nephropelographic phase (at 15 seconds, and 1, 3, and 5 minutes) using coronal 3D T1-weighted gradient echo (GRE) sequences. This sequence can be repeated until the ureters and bladder opacify completely. Upon completion of the above-mentioned sequences, multislice heavily T2-weighted and 3D T1-weighted images are reconstructed by multiplanar reconstruction (MPR) and converted by MIP to generate i.v. urogram-like images. However, with this MRU technique it is not feasible to visualize the renal vasculature and collecting system concurrently since there is not enough contrast available in the renal arteries at the renal excretory phase of the contrast. In addition, if serial postcontrast scans are obtained, it is possible to measure differential renal function and create time-signal intensity curves similar to those used in scintigraphy.

With split-bolus MRU, the aforementioned MRU technique can be modified by splitting the i.v. gadolinium dose. Following the precontrast MRU sequence, only one third of the total contrast dose is given with the furosemide and 3D T1-weighted gradient GRE sequence is implemented to obtain arteriographic phase images.

Five to ten minutes after the first contrast injection (when urinary collecting system visualization is sufficient on T1-weighted MRU images), the second dose of i.v. contrast medium is administered (two-thirds of the total dose). The urinary system is examined again in the coronal plane during the arterial and venous phase by repeating the 3D T1-weighted GRE sequences to image the renal vasculature and collecting system. Following these, dynamic scan, MPR, and MIP images are generated. Fig. 3 provides an imaging scheme for the split-bolus MRU technique. Total study time is about 40–45 minutes; additional 30 minutes is necessary for post-processing. It would be possible to calculate differential renal function by acquiring serial scans after the first dose of gadolinium, but this increases the study time further. Regarding functional assessment, some researchers suggested that as low as one fourth of total dose of gadolinium eliminates the T2* effect and gives more consistent functional results (6). Therefore, we think lower amount of i.v. contrast would not be a disadvantage for functional estimation. Similar to functional imaging, the authors' experience suggests that splitting contrast dose provided diagnostic angiographic and urographic images.

Two discrete boluses of i.v. contrast medium are administered at separate times. First, one-third dose of i.v. contrast is used to image

Main points

- MR urography can provide both morphologic and functional information about urinary tract by using two-dimensional and three-dimensional T1- and T2-weighted sequences.
- With split-bolus MR urography, two discrete boluses of intravenous (i.v.) contrast medium are administered at separate times.
- First dose of i.v. contrast allows imaging the urinary tract at different phases including vascular, parenchymal, and excretory phases. Second dose of i.v. contrast with scanning at arterial and venous phases provides both vascular and excretory phase information.
- This method provides synchronous visualization of vascular and excretory phase enhancement, and can be used to illustrate pathologies such as the nutcracker syndrome, crossing renal vessels and retroiliac ureters that may be responsible for obstruction of the urinary collecting system.



Figure 1. Coronal MIP image of T1-weighted excretory MRU shows left ureteropelvic junction stenosis and mild hydronephrosis.

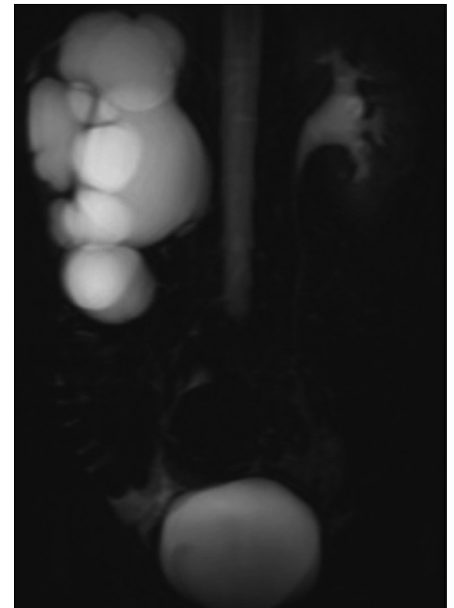


Figure 2. Coronal thick-slab T2-weighted MRU reveals right ureteropelvic junction stenosis and severe hydronephrosis.

the urinary tract at different phases including vascular, parenchymal, and excretory phases. Second, the remaining two-thirds dose of i.v. contrast is used while scanning at the arterial and venous phase to provide both vascular and excretory phase information. Kidneys can concentrate the i.v. contrast medium in up to 200 times of the plasma level; therefore we prefer to split the dose into an initial one-third followed by a two-thirds bolus. This method provides synchronous visualization of vascular and excretory phase enhancement, and can be used to determine pathologies such as the nut-

cracker syndrome, crossing renal vessels, and retroiliac ureters that may be responsible for the urinary collecting system obstruction.

Applications of split-bolus MRU

Crossing renal vessels

Although congenital ureteropelvic junction (UPJ) obstruction is usually secondary to abnormal musculature of the UPJ, in patients with UPJ obstruction, the percentage of crossing vessels has been estimated to be as high as 79% (7). Crossing vessels

may be a prominent artery, vein, or both. They are most commonly located anterior to the UPJ, but posteriorly crossing vessels can also be seen (7). Crossing vessels at the level of UPJ can cause or worsen obstruction and complicate endoscopic management.

Differentiation between the anterior and posterior vessels or identification of the small vein in contact with the UPJ is a frequent problem in diagnosis and management of crossing renal vessels (5, 8–10). The success rate of the endoscopic treatment method significantly drops in the presence of a crossing vessel. In addition, an unrecognized crossing vessel can also result in significant hemorrhage during endoscopic procedure (11). Accurate preoperative identification of a crossing vessel is crucial for the appropriate treatment approach (5, 9–11). Although there are some important signs like hooked or deformed upper ureter in diagnosis of the crossing vessel in i.v. urography, conventional MRI, MRU, and split-bolus MRU can provide excellent simultaneous 3D visualization of the crossing renal vessel and its relationship with the urinary collecting system (Figs. 4–6).

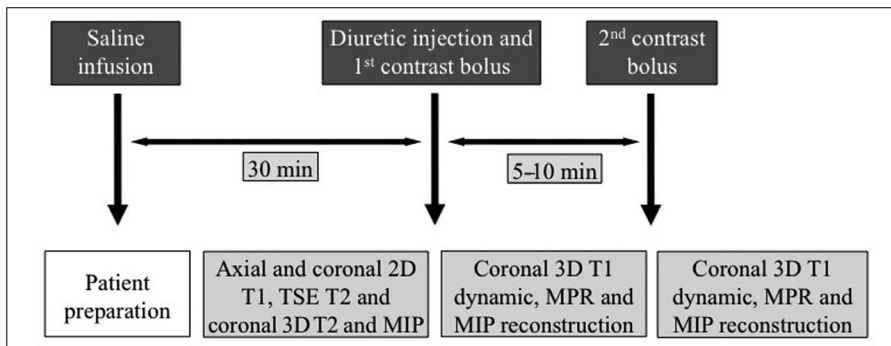


Figure 3. Scheme of the split-bolus MRU technique. 2D, two-dimensional; TSE, turbo spin-echo; 3D, three-dimensional; MIP, maximum intensity projection; MPR, multiplanar reconstruction.

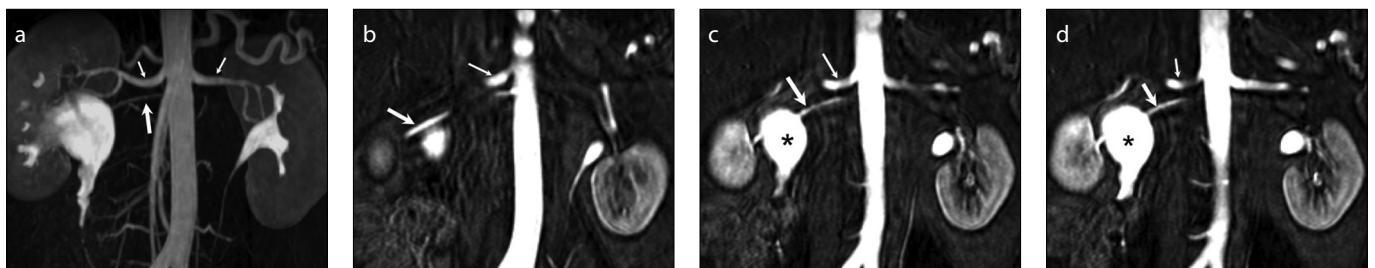


Figure 4. a–d. A 13-year-old girl with right ureteropelvic junction (UPJ) stenosis. A coronal MIP image (a) obtained from second bolus excretory urographic data demonstrates simultaneous enhancement of the collecting system and renal arteries including a right accessory renal artery (*thick arrow*) without close relation with right UPJ. Three consecutive coronal images (b–d) obtained during the arterial phase of the second bolus of contrast medium show concurrent enhancement of the collecting system (*asterisks*) and renal arteries. A right accessory renal artery (*thick arrow*) is not the cause or the exacerbating factor for UPJ stenosis (*thin arrows indicate renal arteries*).

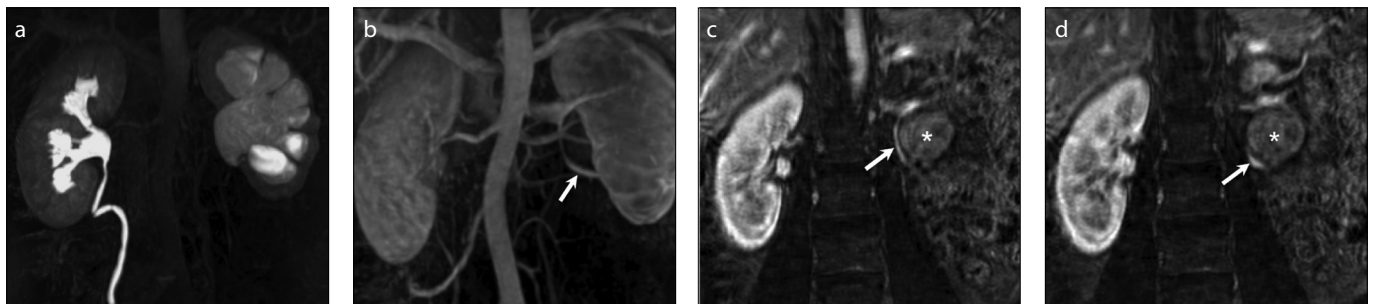


Figure 5. a–d. A 17-year-old male with surgically proven left UPJ stenosis with crossing renal vein. A coronal MIP image (a) obtained from the first bolus excretory urographic data shows the left UPJ stenosis. Coronal dynamic series (b) obtained during the late arterial/venous phase of the first bolus of contrast reveal a pair of left renal veins, the lower one of which (*arrow*) passes close to UPJ. Two consecutive coronal images (c, d) obtained during the arterial phase of the second bolus of contrast medium show concurrent enhancement of the collecting system (*asterisk*) and renal veins. A crossing renal vein (*arrow*) is in close contact with the UPJ and may complicate the surgical intervention.

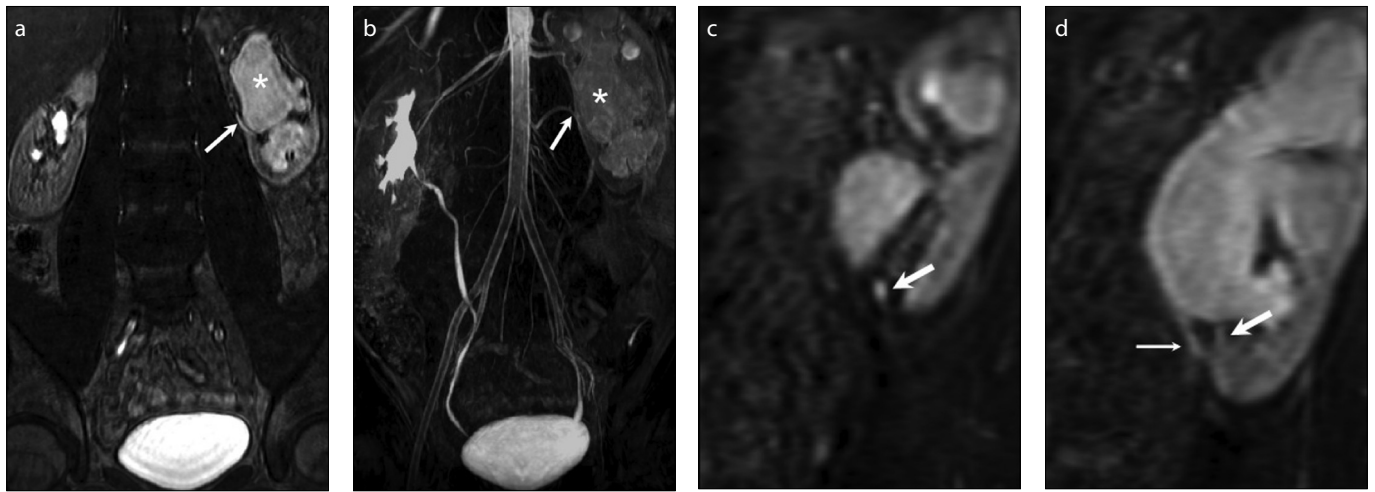


Figure 6. a–d. A two-year-old boy with left UPJ stenosis related with an accessory renal artery. Coronal dynamic series (a) obtained during the arterial phase of the second bolus show simultaneous enhancement of the collecting system (*asterisk*) and the crossing accessory renal artery (*thick arrow*). A coronal MIP image (b) generated from the second bolus excretory urographic data reveals crossing accessory renal artery (*thick arrow*). Two consecutive sagittal reformatted images (c, d) obtained from the second bolus show that the accessory crossing renal artery (*thick arrow*) is not the cause of UPJ (*thin arrow*) stenosis. But awareness of its location is essential during endoureterotomy.

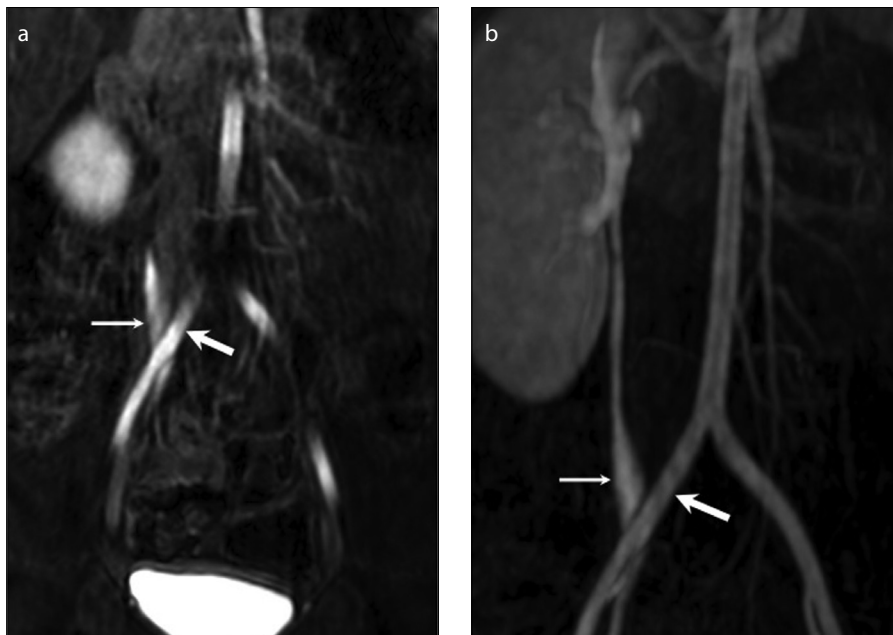


Figure 7. a, b. Retroiliac ureter in a two-year-old boy with left renal agenesis. Coronal dynamic series (a) obtained from the second bolus of intravenous contrast medium and corresponding coronal MIP images (b) show a right retroiliac ureter (*thin arrow*) with mild dilatation (*thick arrow* indicates common iliac artery).

Retroiliac ureters

Retroiliac ureter is a rare congenital cause of noncalculous low ureteral obstruction, and it is mostly unilateral. This entity occurs due to faulty migration of the kidney during embryologic development. Retroiliac location of the ureter may lead to infection or hematuria due to venous congestion of the ureteral mucosa by the external arterial compression. Pre-operative diagnosis of this entity is usual-

ly challenging and requires high level of suspicion (Fig. 7). A retroiliac ureter should be suspected in patients with varying degrees of upper urinary tract dilatation, especially if the diagnosis is undetermined in excretory urography and ultrasonography (12). Split-bolus MRU technique provides precise diagnosis by simultaneous 3D visualization of the compressed ureter and compressing iliac artery, and abnormal course of the ureter behind the iliac artery.

Nutcracker phenomenon/syndrome

Nutcracker phenomenon, also called the left renal vein (LRV) entrapment, is characterized by impeded outflow from the LRV accompanied by distension of the distal portion of the vein. The nutcracker syndrome is the clinical equivalent of nutcracker phenomenon characterized by symptoms varying from asymptomatic microhematuria to severe pelvic congestion (13).

There are two types of nutcracker syndrome. In the most common type, also known as the anterior nutcracker syndrome, the LRV is compressed between the aorta and superior mesenteric artery. In the less common type, also known as the posterior nutcracker syndrome, the retro-aortic or circum-aortic LRV is compressed between the aorta and the vertebral body. Diagnosis of the nutcracker syndrome is difficult and frequently delayed (13, 14). Split-bolus MRU can provide excellent simultaneous 3D demonstration of urinary collecting system, arterial structures (aorta and superior mesenteric artery), renal venous structures (in general arterial phase provides sufficient enhancement of the renal veins to diagnose the renal vein abnormalities), and surrounding soft tissue and bony structures (Fig. 8).

Ovarian vein syndrome

Ovarian vein syndrome is a relatively rare and probably underdiagnosed condition. In this syndrome, a dilated ovarian vein compressing the ureter leads to its stenosis or obstruction, and dilatation of the collecting

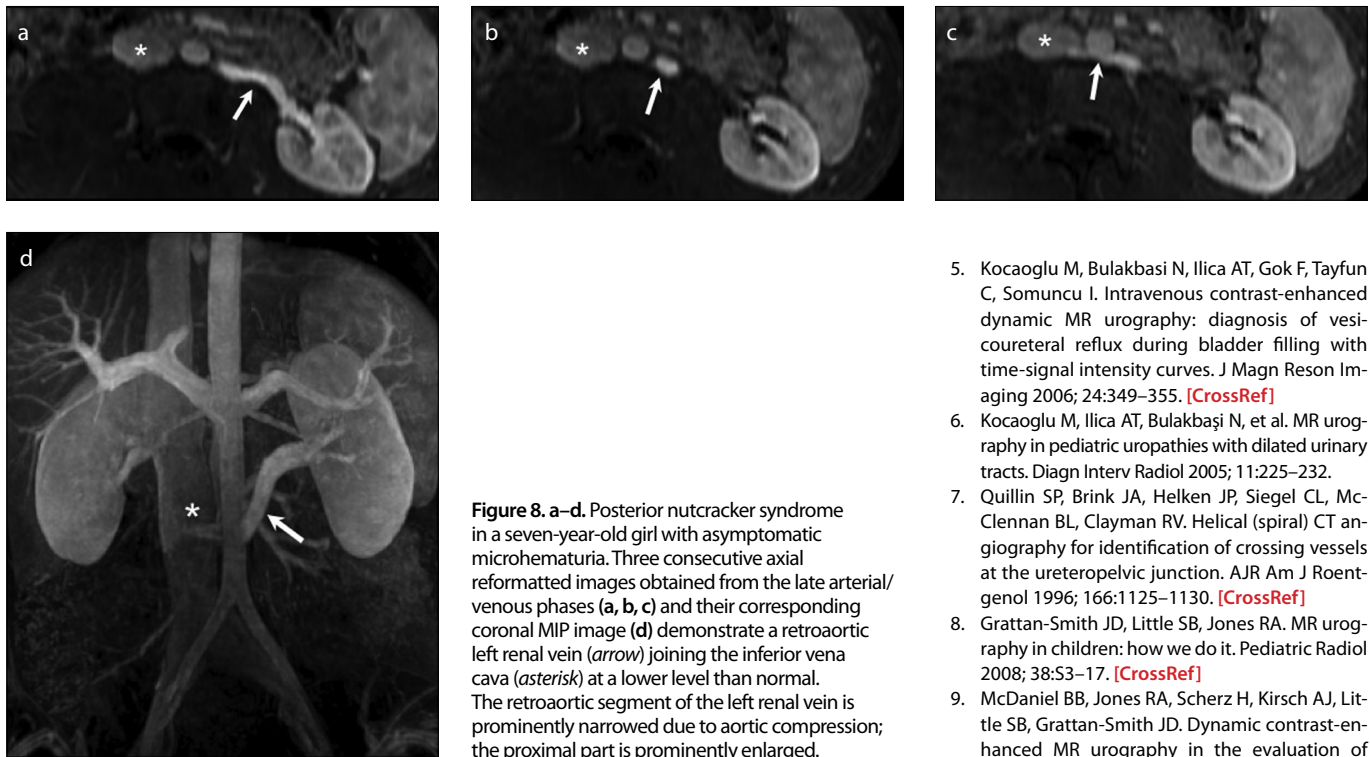


Figure 8. a–d. Posterior nutcracker syndrome in a seven-year-old girl with asymptomatic microhematuria. Three consecutive axial reformatted images obtained from the late arterial/venous phases (**a, b, c**) and their corresponding coronal MIP image (**d**) demonstrate a retroaortic left renal vein (*arrow*) joining the inferior vena cava (*asterisk*) at a lower level than normal. The retroaortic segment of the left renal vein is prominently narrowed due to aortic compression; the proximal part is prominently enlarged.

system. The most important etiologic factor is parity, which is associated with ovarian vein reflux, dilation and varicosity of the ovarian vein, or ovarian vein thrombosis. Ovarian vein syndrome is an extremely rare condition in a child (15).

The right ovarian vein is the most frequently affected, although this entity can also affect the left side or both sides. Imaging studies such as i.v. urography, ultrasonography, CT, or MRI supports the diagnosis; but it remains a diagnosis of exclusion of other conditions causing similar symptoms (15). Split-bolus MRU can show simultaneous visualization of the compressed ureter and enlarged ovarian vein.

Conclusion

It is essential to select the accurate imaging technique to evaluate a specific clinical condition. By splitting the contrast medium into two separate bolus injections, MRU can

demonstrate the urinary collecting system and vessels simultaneously, and allow preoperative radiologic diagnosis of obstructing vessel noninvasively and without radiation exposure.

References

1. Levendeker JR, Barnes CE, Zagoria RJ. MR urography: techniques and clinical applications. *Radiographics* 2008; 28:23–46. [\[CrossRef\]](#)
2. Battal B, Kocaoglu M, Akgun V, Aydur E, Dayanc M, Ilica T. Feasibility of MR urography in patients with urinary diversion. *J Med Imaging Radiat Oncol* 2011; 55:542–550. [\[CrossRef\]](#)
3. Koçyigit A, Yüksel S, Bayram R, Yılmaz İ, Karabulut N. Efficacy of magnetic resonance urography in detecting renal scars in children with vesicoureteral reflux. *Pediatr Nephrol* 2014; 29:1215–1220. [\[CrossRef\]](#)
4. Kocycigit A, Serinken M, Ceven Z, et al. A strategy to optimize CT use in children with mild blunt head trauma utilizing clinical risk stratification; could we improve CT use in children with mild head injury? *Clin Imaging* 2014; 38:236–240. [\[CrossRef\]](#)

5. Kocaoglu M, Bulakbasi N, Ilica AT, Gok F, Tayfun C, Somuncu I. Intravenous contrast-enhanced dynamic MR urography: diagnosis of vesicoureteral reflux during bladder filling with time-signal intensity curves. *J Magn Reson Imaging* 2006; 24:349–355. [\[CrossRef\]](#)
6. Kocaoglu M, Ilica AT, Bulakbaşı N, et al. MR urography in pediatric uropathies with dilated urinary tracts. *Diagn Interv Radiol* 2005; 11:225–232.
7. Quillin SP, Brink JA, Helken JP, Siegel CL, McClellan BL, Clayman RV. Helical (spiral) CT angiography for identification of crossing vessels at the ureteropelvic junction. *AJR Am J Roentgenol* 1996; 166:1125–1130. [\[CrossRef\]](#)
8. Grattan-Smith JD, Little SB, Jones RA. MR urography in children: how we do it. *Pediatric Radiol* 2008; 38:S3–17. [\[CrossRef\]](#)
9. McDaniel BB, Jones RA, Scherz H, Kirsch AJ, Little SB, Grattan-Smith JD. Dynamic contrast-enhanced MR urography in the evaluation of pediatric hydronephrosis: Part 2, anatomic and functional assessment of ureteropelvic junction obstruction. *AJR Am J Roentgenol* 2005; 185:1608–1614. [\[CrossRef\]](#)
10. Braun P, Guilbert JP, Kazmi F. Multidetector computed tomography arteriography in the preoperative assessment of patients with ureteropelvic junction obstruction. *Eur J Radiol* 2007; 61:170–175. [\[CrossRef\]](#)
11. Wang W, LeRoy AJ, McKusick MA, Segura JW, Patterson DE. Detection of crossing vessels as the cause of ureteropelvic junction obstruction: the role of antegrade pyelography prior to endopyelotomy. *J Vasc Interv Radiol* 2004; 15:1435–1441. [\[CrossRef\]](#)
12. Kocaoglu M, Gok F, Kibar Y, Battal B. Retroiliac ureters with bilateral testicular microlithiasis: simultaneous MDCT visualization of ureters and iliac arteries with biphasic contrast injection. *AJR Am J Roentgenol* 2007; 188:W390–391. [\[CrossRef\]](#)
13. Kurklinsky AK, Rooke TW. Nutcracker phenomenon and nutcracker syndrome. *Mayo Clin Proc* 2010; 85:552–559. [\[CrossRef\]](#)
14. Kraus GJ, Goerzer HG. MR-angiographic diagnosis of an aberrant retroaortic left renal vein and review of the literature. *Clin Imaging* 2003; 2:132–134. [\[CrossRef\]](#)
15. Pui M. Imaging of vascular disorders of the female pelvis. *Australas Radiol* 2006; 50:405–411. [\[CrossRef\]](#)